Density waves in the full velocity difference model

2006 J. Phys. A: Math. Gen. 39 1251

(http://iopscience.iop.org/0305-4470/39/6/003)

INSTITUTE OF PHYSICS PUBLISHING JOURNAL OF PHYSICS A: MATHEMATICAL AND GENERAL

J. Phys. A: Math. Gen. **39** (2006) 1251–1263 doi:10.1088/0305-4470/39/6/003

Density waves in the full velocity difference model

Zhong-Hui Ou, Shi-Qiang Dai and Li-Yun Dong

Shanghai Institute of Applied Mathematics and Mechanics, Shanghai University, Shanghai 200072, People's Republic of China

E-mail: ouzhonghui@vip.sina.com

Received 27 October 2005, in final form 22 December 2005
Published 25 January 2006
Online at stacks.iop.org/JPhysA/39/1251

Abstract

Density waves are investigated in the full velocity difference model (FVDM) analytically and numerically. By the use of nonlinear analysis, the Burgers, Korteweg–de Vries (KdV) and Modified KdV equations are derived for the triangular shock wave, the soliton wave and the kink–antikink wave, respectively, appearing in the stable region out of the coexisting curve, near the spinodal line, and in the unstable region within the spinodal line. It is shown, numerically, that the triangular shock wave and the soliton wave are determined by the initial perturbation configuration and different initial perturbations will produce different waveforms in the stable region or near the spinodal line.

PACS numbers: 05.90.+m, 47.35.+i, 89.40.+k

1. Introduction

Traffic flow problems have attracted much attention with considerable interest for decades. When car density is higher than the critical density in a highway, traffic jams occur and propagate as density waves [1–6]. Kerner and Konhäuser found the single-pulse density wave in numerical simulations of the cluster with the hydrodynamic traffic flow model [7], which was lately recognized as the asymmetric kink–antikink density wave. Kurtze and Hong derived the KdV equation from the hydrodynamic model by using nonlinear analysis and obtained the soliton solution [8]. Komatsu and Sasa derived the MKdV equation from the optimal velocity model (OVM) [3, 9]. Recently, Muramatsu and Nagatani clarified the difference between the soliton and kink density waves [10] and found the triangular shock wave described by the Burgers equation during the relaxation process of nonuniform density profile in the stable traffic flow to the uniform density profile [11]. Up to now, three types of density waves have all been found in traffic flow: the first is the kink–antikink density described by the MKdV equation appearing in the unstable region within the spinodal line, the second is the soliton density wave described by the KdV equation appearing near the spinodal line and the third

is the triangular shock wave described by the Burgers equation appearing in the stable region out of the coexisting curve [11–16].

The typical nonlinear wave equations are often derived from the OVM [2–4, 9, 10, 14, 15]. Helbing and Tilch carried out a calibration of the OVM with respect to the empirical data and it is shown that the OVM encountered the problems of too high acceleration and unrealistic deceleration [17]. In order to solve this problem, Helbing introduced the negative velocity difference term into the OVM and proposed a generalized force model (GFM) [17]. Jiang considered that the GFM does not take the effect of the positive velocity difference on traffic dynamics into account, which would result into the GFMs invalidation in anticipating the delay time and disturbance propagation velocity [18]. In order to solve the problem, Jiang takes both positive and negative velocity differences into account and proposed the FVDM [18]. The work of this paper is to derive the nonlinear equations from the FVDM and determine the relations between initial conditions and density waves in numerical simulations.

In this paper, the nonlinear analysis is applied to the FVDM. The Burgers, the KdV and the MKdV equations are derived from the FVDM. We take numerical simulations on three kinds of nonlinear density waves with different initial conditions [10, 11, 15, 16]. Finally, we discuss the physical significance of the nonlinear density waves.

2. Density waves and nonlinear equations

In 1995, Bando *et al* presented a car-following model called the optimal velocity model [2–4]. It was based on the idea that each vehicle has an optimal velocity, which depends on the following distance of the preceding vehicle. The equation of the model is

$$\frac{\mathrm{d}^2 x_n(t)}{\mathrm{d}t^2} = a\left[V(\triangle x_n(t)) - \frac{\mathrm{d}x_n(t)}{\mathrm{d}t}\right], \tag{1}$$

where $x_n(t)$ is the position of car n at time t, $\triangle x_n(t)$ $(= x_{n+1}(t) - x_n(t))$ is the headway of the car n at time t, V is the optimal velocity that the drivers prefer and a is the sensitivity of a driver.

Jiang took the effect of the velocity difference on traffic dynamics into account, added a term on the right-hand side of equation (1) and obtained the FVDM

$$\frac{\mathrm{d}^2 x_n(t)}{\mathrm{d}t^2} = a\left[V(\triangle x_n(t)) - \frac{\mathrm{d}x_n(t)}{\mathrm{d}t}\right] + \lambda a \frac{\mathrm{d}\triangle x_n(t)}{\mathrm{d}t}, \tag{2}$$

where λ is the responsive factor of velocity difference [18]. If $\lambda = 0$, equation (2) can be reduced to equation (1). In this paper, we nonlinearly analyse the FVDM and derive the nonlinear wave equations from the FVDM to describe the density waves.

2.1. Linear stability analysis

The linear stability theory is applied to the FVDM in this subsection. We consider the stability of a uniform traffic flow. The uniform traffic flow is defined by such a case that all cars move with constant headway $\triangle x^{(0)}$ and optimal velocity $V(\triangle x^{(0)})$. The solution of the uniform steady state is given by

$$x_n^{(0)} = \triangle x^{(0)} n + V(\triangle x^{(0)})t, \qquad \triangle x^{(0)} = L/N, \tag{3}$$

where N is the number of cars, L is the system size and $\triangle x^{(0)}$ is the car spacing (identical headway).

Let $y_n(t)$ be small deviations from the uniform solution $x_n^{(0)}$: $x_n(t) = x_n^{(0)}(t) + y_n(t)$. Then, the linearized equation is obtained from equation (2),

$$\frac{\mathrm{d}^2 y_n(t)}{\mathrm{d}t^2} = a\left[V'(\triangle x^{(0)})\triangle y_n(t) - \frac{\mathrm{d}y_n(t)}{\mathrm{d}t}\right] + \lambda a\frac{\mathrm{d}\triangle y_n(t)}{\mathrm{d}t}, \tag{4}$$

where $V'(\triangle x^{(0)}) = [\mathrm{d}V(\triangle x)/\mathrm{d}\triangle x]|_{\triangle x=\triangle x^{(0)}}$.

By expanding $y_n(t) = Y\exp(\mathrm{i}\alpha_\mathrm{k} n + zt)$, one obtains

$$z^2 + [a + \lambda a - \lambda a\exp(\mathrm{i}\alpha_\mathrm{k})]z - aV'[\exp(\mathrm{i}\alpha_\mathrm{k}) - 1] = 0, \tag{5}$$

where $z = u + \mathrm{i}v$ (u and v are real). When $u = 0$, the critical curve is

$$V' = \lambda a(1 + \lambda - \lambda\cos\alpha_\mathrm{k}) + \frac{a}{2\cos^2\frac{\alpha_\mathrm{k}}{2}}(1 + \lambda - \lambda\cos\alpha_\mathrm{k})^2. \tag{6}$$

The traffic flow is stable if the following condition is satisfied:

$$V'(\triangle x^{(0)}) < \frac{a(2\lambda + 1)}{2}. \tag{7}$$

2.2. *Burgers equation*

The Burgers equation is derived for the density wave in the stable traffic flow region in this subsection. We now consider long-wave modes on coarse-grained scales by the long-wave expansion and the slowly varying behaviour at long wavelengths in the stable region. We extract slow scales for space variable n and time variable t and define slow variables X and T for $0 < \varepsilon \ll 1$ [11, 19]:

$$X = \varepsilon(n + bt) \qquad \text{and} \qquad T = \varepsilon^2 t, \tag{8}$$

where b is a constant determined later. The headway is set as

$$\triangle x_n(t) = \triangle x^{(0)} + \varepsilon R(X, T). \tag{9}$$

For later convenience, equation (2) is rewritten as

$$\frac{\mathrm{d}^2\triangle x_n(t)}{\mathrm{d}t^2} = a\left[V(\triangle x_{n+1}(t)) - V(\triangle x_n(t)) - \frac{\mathrm{d}\triangle x_n(t)}{\mathrm{d}t}\right] + \lambda a\left(\frac{\mathrm{d}\triangle x_{n+1}(t)}{\mathrm{d}t} - \frac{\mathrm{d}\triangle x_n(t)}{\mathrm{d}t}\right). \tag{10}$$

By expanding each term in equation (10) to the third order of ε with the use of equations (8) and (9), one obtains

$$\frac{\mathrm{d}\triangle x_n(t)}{\mathrm{d}t} = \varepsilon^2 b\partial_X R + \varepsilon^3\partial_T R, \tag{11}$$

$$\frac{\mathrm{d}^2\triangle x_n}{\mathrm{d}t^2} = \varepsilon^3 b^2\partial_X^2 R, \tag{12}$$

$$\triangle x_{n+1}(t) = \triangle x^{(0)} + \varepsilon R + \varepsilon^2\partial_X R + \frac{1}{2}\varepsilon^3\partial_X^2 R, \tag{13}$$

$$V(\triangle x_n) = V(\triangle x^{(0)}) + V'(\triangle x_n - \triangle x^{(0)}) + \frac{1}{2}V''(\triangle x_n - \triangle x^{(0)})^2, \tag{14}$$

$$V(\triangle x_{n+1}) - V(\triangle x_n) = \varepsilon^2 V'\partial_X R + \varepsilon^3\left(V''R\partial_X R + \frac{1}{2}V'\partial_X^2 R\right), \tag{15}$$

$$\frac{\mathrm{d}(\triangle x_{n+1} - \triangle x_n)}{\mathrm{d}t} = \varepsilon^3 b\partial_X^2 R. \tag{16}$$

By substituting equations (11)–(16) into equation (10), one obtains the following nonlinear partial differential equation:

$$\varepsilon^2(b - V')\partial_X R + \varepsilon^3 \left[\partial_T R - V'' R \partial_X R - \left(\frac{V' + 2\lambda b}{2} - \frac{b^2}{a} \right) \partial_X^2 R \right] = 0, \tag{17}$$

where $\partial_T = \partial/\partial T$, $\partial_X = \partial/\partial X$ and $V''(\triangle x^{(0)}) = [\mathrm{d}^2 V(\triangle x)/\mathrm{d}\triangle x^2]|_{\triangle x = \triangle x^{(0)}}$.

By taking $b = V'$, the second-order term of ε is eliminated from equation (17). One obtains the following partial differential equation:

$$\partial_T R - V'' R \partial_X R = \left(\frac{2\lambda + 1}{2} V' - \frac{V'^2}{a} \right) \partial_X^2 R. \tag{18}$$

In the stable traffic region satisfying the stability condition equation (7),

$$\frac{2\lambda + 1}{2} V' - \frac{V'^2}{a} = V' \left(\frac{2\lambda + 1}{2} - \frac{V'}{a} \right) > 0,$$

$V''(\triangle x) < 0$ for $\triangle x > h_c$ (h_c is the safety distance), so equation (18) is the Burgers equation. The solution of the Burgers equation for the asymptotic stage ($T \gg 1$) is a train of N-triangular shock waves and can be given by

$$R(X, T) = \frac{1}{|V''|T} \left[X - \frac{1}{2}(\eta_n + \eta_{n+1}) \right] - \frac{1}{2|V''|T} (\eta_{n+1} - \eta_n) \tanh \left[\frac{B}{4|V''|T} (\eta_{n+1} - \eta_n)(X - \xi_n) \right], \tag{19}$$

where $B = \frac{2\lambda+1}{2} V' - \frac{1}{a} V'^2$ [11, 20]. The coordinates of the shock fronts are given by $\xi_n (n = 1, 2, \ldots, N)$ and those of the intersections of the slopes with the x axis by $\eta_n (n = 1, 2, \ldots, N)$. When $\lambda = 0$, $B = \frac{1}{2} V' - \frac{1}{a} V'^2$ is the result derived from the OVM [11, 16].

2.3. KdV equation

By expanding equation (5) with $\mathrm{i}\alpha_k$ near the neutral stability point $(\triangle x^{(0)}, a_s)$, $a_s = \frac{2}{2\lambda+1} V'$, one obtains

$$z = \mathrm{i} \frac{(2\lambda + 1)a_s}{2} \alpha_k + \frac{(2\lambda + 1)(a_s - a)}{4} \alpha_k^2 - \mathrm{i} \frac{(2\lambda + 1)a_s}{12} \alpha_k^3 - \frac{(2\lambda + 1)a_s}{16} \alpha_k^4 + O(\alpha_k^5). \tag{20}$$

Suppose the headway of uniform traffic is near the neutral stability point. We quantify this by writing

$$\begin{aligned} &V'(\triangle x^{(0)}) - \frac{2\lambda + 1}{2}(a_s - \delta a) = \frac{2\lambda + 1}{2} \delta a = \frac{2\lambda + 1}{2} a \left(\frac{a_s}{a} - 1 \right), \\ &\frac{2\lambda + 1}{2} a \left| \frac{a_s}{a} - 1 \right| \equiv \beta \varepsilon^2, \qquad \beta = \frac{2\lambda + 1}{2} a, \qquad \varepsilon = \sqrt{\left| \frac{a_s}{a} - 1 \right|}. \end{aligned} \tag{21}$$

ε is introduced as a small scaling parameter.

We derive the KdV equation from equation (2) near the spinodal line (the neutral stability line) in this subsection. One defines the slow variables X and T [8, 9, 12, 14, 19]:

$$X = \varepsilon(n + bt) \qquad \text{and} \qquad T = \varepsilon^3 t. \tag{22}$$

The headway is set as [10, 11]

$$\triangle x_n(X, T) = \triangle x^{(0)} + \varepsilon^2 R(X, T). \tag{23}$$

By expanding each term in equation (10) to the sixth order of ε, one obtains

$$\frac{\mathrm{d}\triangle x_n}{\mathrm{d}t} = \varepsilon^3 b\partial_X R + \varepsilon^5 \partial_T R, \tag{24}$$

$$\frac{\mathrm{d}^2\triangle x_n}{\mathrm{d}t^2} = \varepsilon^4 b^2 \partial_X^2 R + 2\varepsilon^6 b\partial_X \partial_T R, \tag{25}$$

$$\triangle x_{n+1}(t) = \triangle x^{(0)} + \varepsilon^2 R + \varepsilon^3 \partial_X R + \frac{1}{2}\varepsilon^4 \partial_X^2 R + \frac{1}{6}\varepsilon^5 \partial_X^3 R + \frac{1}{24}\varepsilon^6 \partial_X^4 R, \tag{26}$$

$$V(\triangle x_n) = V(\triangle x^{(0)}) + V'(\triangle x_n - \triangle x^{(0)}) + \frac{1}{2}V''(\triangle x_n - \triangle x^{(0)})^2, \tag{27}$$

$$\begin{aligned} V(\triangle x_{n+1}) - V(\triangle x_n) = {} & \varepsilon^3 V'\partial_X R + \frac{1}{2}\varepsilon^4 V'\partial_X^2 R + \varepsilon^5\left(\frac{V'}{6}\partial_X^3 R + V''R\partial_X R\right) \\ & + \varepsilon^6\left(\frac{V'}{24}\partial_X^4 R + \frac{V''}{4}\partial_X^2 R^2\right). \end{aligned} \tag{28}$$

$$\frac{\mathrm{d}(\triangle x_{n+1} - \triangle x_n)}{\mathrm{d}t} = \varepsilon^4 b\partial_X^2 R + \frac{1}{2}\varepsilon^5 b\partial_X^3 R + \varepsilon^6\left(\partial_X\partial_T R + \frac{1}{6}b\partial_X^4 R\right). \tag{29}$$

By substituting equations (24)–(29) into equation (10), one obtains the following nonlinear partial differential equation:

$$\begin{aligned} & \varepsilon^3(ab - aV')\partial_X R + \varepsilon^4\left(b^2 - \frac{aV'}{2} - \lambda ab\right)\partial_X^2 R \\ & \quad + \varepsilon^5\left(a\partial_T R - \frac{aV'}{6}\partial_X^3 R - aV''R\partial_X R - \frac{\lambda ab}{2}\partial_X^3 R\right) \\ & \quad + \varepsilon^6\left(2b\partial_X\partial_T R - \frac{aV'}{24}\partial_X^4 R - \frac{aV''}{4}\partial_X^2 R^2 - \lambda a\partial_X\partial_T R - \frac{\lambda ab}{6}\partial_X^4 R\right) = 0. \end{aligned} \tag{30}$$

By taking $b = V'$, the third-order term of ε is eliminated and the forth-order term of ε changes into

$$\varepsilon^4\left(b^2 - \frac{aV'}{2} - \lambda ab\right)\partial_X^2 R = \pm\varepsilon^6\beta V'\partial_X^2 R. \tag{31}$$

Using the fifth-order term of ε in equation (30),

$$a\partial_T R - \frac{aV'}{6}\partial_X^3 R - aV''R\partial_X R - \frac{\lambda ab}{2}\partial_X^3 R = a\partial_T R - \frac{(3\lambda+1)aV'}{6}\partial_X^3 R - \frac{aV''}{2}\partial_X R^2,$$

one obtains

$$\partial_X\partial_T R = \frac{(3\lambda+1)V'}{6}\partial_X^4 R + \frac{V''}{2}\partial_X^2 R^2 + O(\varepsilon). \tag{32}$$

By taking equations (31) and (32) into equation (30), one obtains

$$\begin{aligned} & \varepsilon^5\left[a\partial_T R - \left(\frac{aV'}{6} + \frac{\lambda ab}{2}\right)\partial_X^3 R - aV''R\partial_X R\right] + \varepsilon^6\left[\pm\beta V'\partial_X^2 R\right. \\ & \quad \left. + \left(\frac{(2b-\lambda a)(3\lambda+1) - \lambda a}{6} - \frac{a}{24}\right)V'\partial_X^4 R + \frac{4V' - (2\lambda+1)a}{4}V''\partial_X^2 R^2\right] = 0. \end{aligned} \tag{33}$$

In order to derive the regularized equation, we make the following transformations:

$$R = \frac{|g|}{V''}R', \qquad X = -\sqrt{\frac{(3\lambda+1)V'}{6|g|}}X' \qquad \text{and} \qquad T = \sqrt{\frac{(3\lambda+1)V'}{6|g|^3}}T', \tag{34}$$

where g is a negative constant. With the use of equation (34), one obtains the regularized equation

$$\varepsilon^5 \frac{ag^2}{V''}\sqrt{\frac{6|g|}{(3\lambda+1)V'}}(\partial_{T'}R' + \partial_{X'}^3 R' + R'\partial_{X'}R') + \varepsilon^6 \frac{6g^2}{(3\lambda+1)V'V''}\left[A_1\partial_{X'}^2 R' + A_2\partial_{X'}^4 R' + A_3\partial_{X'}^2 R'^2\right] = 0, \tag{35}$$

where

$$A_1 = \pm\beta V',$$
$$A_2 = |g|\frac{4(2b-\lambda a)(3\lambda+1) - 4\lambda a - a}{4(3\lambda+1)} \simeq \frac{3a|g|(2\lambda+1)^2}{4(3\lambda+1)},$$
$$A_3 = |g|\left(V' - \frac{2\lambda+1}{4}a\right) \simeq a|g|\frac{2\lambda+1}{4}.$$

If one ignores the $O(\varepsilon^6)$ terms in equation (35), it is just the KdV equation with a soliton solution as the desired solution,

$$R_0'(X', T') = A\,\mathrm{sech}^2\left[\sqrt{\frac{A}{12}}\left(X' - \frac{A}{3}T'\right)\right]. \tag{36}$$

Amplitude A of soliton solutions of the KdV equation is a free parameter. The perturbation term $O(\varepsilon^6)$ of perturbed KdV equation, equation (35), selects a unique member of the continuous family of KdV solitons.

Next, assuming that $R'(X', T') = R_0'(X', T') + \varepsilon R_1'(X', T')$, we take into account the $O(\varepsilon)$ correction. In order to determine the selected value of A for the soliton solution equation (36), it is necessary to satisfy the solvability condition,

$$(R_0', M[R_0']) \equiv \int_{-\infty}^{\infty} R_0' M[R_0']\,\mathrm{d}X' = 0, \tag{37}$$

where $M[R_0']$ is the $O(\varepsilon^6)$ term of equation (35).

By performing the integration, one obtains the selected value

$$A = \frac{21A_1}{5A_2 - 24A_3} = \frac{14(3\lambda+1)V'}{(14\lambda+3)|g|}. \tag{38}$$

By rewriting each variable to the original one, one obtains the soliton solution of the headway:

$$\triangle x_n = \triangle x^{(0)} + \left|\frac{a_s}{a} - 1\right|\frac{14(3\lambda+1)V'}{(14\lambda+3)V''}\,\mathrm{sech}^2 \times \left\{-\sqrt{\frac{7|a_s/a-1|}{14\lambda+3}}\left[n + \left(1 + \frac{14(3\lambda+1)}{3(14\lambda+3)}\left|\frac{a_s}{a} - 1\right|\right)V't\right]\right\}. \tag{39}$$

When $\lambda = 0$, $A = \frac{14V'}{3|g|}$ is the result derived from the OVM [10, 11, 15].

2.4. MKdV equation

The MKdV equation is derived in the unstable region just below the critical point (h_c, a_c), $V''(h_c) = 0$ in this subsection [9, 11, 15]. The slow variables have been defined by equation (22). The headway is set as follows:

$$\triangle x_n = h_c + \varepsilon R(X, T), \qquad \varepsilon = \sqrt{\frac{a_c}{a} - 1} \ll 1. \tag{40}$$

By expanding each term in equation (10) to the fifth order of ε, one obtains

$$\frac{\mathrm{d}\triangle x_n}{\mathrm{d}t} = \varepsilon^2 b\partial_X R + \varepsilon^4 \partial_T R, \tag{41}$$

$$\frac{\mathrm{d}^2\triangle x_n}{\mathrm{d}t^2} = \varepsilon^3 b^2 \partial_X^2 R + 2\varepsilon^5 b\partial_X \partial_T R, \tag{42}$$

$$\triangle x_{n+1}(t) = h_\mathrm{c} + \varepsilon R + \varepsilon^2 \partial_X R + \frac{1}{2}\varepsilon^3 \partial_X^2 R + \frac{1}{6}\varepsilon^4 \partial_X^3 R + \frac{1}{24}\varepsilon^5 \partial_X^4 R, \tag{43}$$

$$V(\triangle x_n) = V(h_\mathrm{c}) + V'(\triangle x_n - h_\mathrm{c}) + \frac{1}{6}V'''(\triangle x_n - h_\mathrm{c})^3, \tag{44}$$

$$\begin{aligned} V(\triangle x_{n+1}) - V(\triangle x_n) = {} & \varepsilon^2 V'\partial_X R + \frac{1}{2}\varepsilon^3 V'\partial_X^2 R + \varepsilon^4\left(\frac{V'}{6}\partial_X^3 R + \frac{V'''}{6}R\partial_X R\right) \\ & + \varepsilon^5\left(\frac{V'}{24}\partial_X^4 R + \frac{V'''}{12}\partial_X^2 R^3\right). \end{aligned} \tag{45}$$

$$\frac{\mathrm{d}(\triangle x_{n+1} - \triangle x_n)}{\mathrm{d}t} = \varepsilon^3 b\partial_X^2 R + \frac{1}{2}\varepsilon^4 b\partial_X^3 R + \varepsilon^5\left(\partial_X\partial_T R + \frac{1}{6}b\partial_X^4 R\right). \tag{46}$$

By substituting equations (41)–(46) into equation (10), one obtains the following nonlinear partial differential equation:

$$\begin{aligned} & \varepsilon^2(ab - aV')\partial_X R + \varepsilon^3\left(b^2 - \frac{aV'}{2} - \lambda ab\right)\partial_X^2 R \\ & \quad + \varepsilon^4\left[a\partial_T R - \left(\frac{aV'}{6} + \frac{\lambda ab}{2}\right)\partial_X^3 R - \frac{aV'''}{6}\partial_X R^3\right] \\ & \quad + \varepsilon^5\left[(2b - \lambda a)\partial_X\partial_T R - \left(\frac{aV'}{24} + \frac{\lambda ab}{6}\right)\partial_X^4 R - \frac{aV'''}{12}\partial_X^2 R^3\right] = 0. \end{aligned} \tag{47}$$

By taking $b = V'$, the second-order term of ε is eliminated and the third-order term of ε may be written as

$$\varepsilon^3\left(b^2 - \frac{aV'}{2} - \lambda ab\right)\partial_X^2 R = \pm\varepsilon^5\beta V'\partial_X^2 R. \tag{48}$$

Using the forth-order term of ε in equation (47),

$$a\partial_T R - \left(\frac{aV'}{6} + \frac{\lambda ab}{2}\right)\partial_X^3 R - \frac{aV'''}{6}\partial_X R^3,$$

one obtains

$$\partial_X\partial_T R = \frac{(3\lambda + 1)V'}{6}\partial_X^4 R + \frac{V'''}{6}\partial_X^2 R^3 + O(\varepsilon). \tag{49}$$

By taking equations (48) and (49) into equation (47), one obtains

$$\begin{aligned} & \varepsilon^4\left(a\partial_T R - \frac{3\lambda + 1}{6}aV'\partial_X^3 R - \frac{aV'''}{6}\partial_X R^3\right) \\ & \quad + \varepsilon^5\left[\pm\beta V'\partial_X^2 R + \frac{4(2b - \lambda a)(3\lambda + 1) - (4\lambda + 1)a}{24}V'\partial_X^4 R\right. \\ & \quad \left. + \frac{2(2b - \lambda a) - a}{12}V'''\partial_X^2 R^3\right] = 0. \end{aligned} \tag{50}$$

In order to derive the regularized equation, we make the following transformations:

$$R = -\sqrt{-\frac{(3\lambda + 1)V'}{V'''}}R', \qquad X = X' \qquad \text{and} \qquad T = \frac{6}{(3\lambda + 1)V'}T'. \tag{51}$$

With the use of equation (51), one obtains the regularized equation

$$-\varepsilon^4 a\frac{(3\lambda+1)V'}{6}\sqrt{-\frac{(3\lambda+1)V'}{V'''}}\left(\partial_{T'}R'-\partial^3_{X'}R'+\partial_{X'}R'^3\right)$$
$$-\varepsilon^5 V'\sqrt{-\frac{(3\lambda+1)V'}{V'''}}\left[C_1\partial^2_{X'}R'+C_2\partial^4_{X'}R'+C_3\partial^2_{X'}R'^3\right]=0, \tag{52}$$

where

$$C_1=\pm\beta,$$
$$C_2=\frac{4(2b-\lambda a)(3\lambda+1)-(4\lambda+1)a}{24}\simeq\frac{4\lambda(\lambda+1)+1}{8}a,$$
$$C_3=-\frac{2(2b-\lambda a)-a}{12}(3\lambda+1)\simeq\frac{(2\lambda+1)(3\lambda+1)}{12}a.$$

If one ignores the $O(\varepsilon^5)$ term in equation (52), it is just the MKdV equation with a kink solution as the desired solution,

$$R_0'(X',T')=\sqrt{C}\tanh\left[\sqrt{\frac{C}{2}}(X'-CT'\right]. \tag{53}$$

Amplitude C of kink–antikink solutions of the MKdV equation is a free parameter. The perturbation term $O(\varepsilon^5)$ of perturbed MKdV equation (52) selects a unique member of the continuous family of MKdV kinks.

Under the solvability condition, one obtains the selected value

$$C=\frac{5C_1}{2C_2-3C_3}=\frac{10}{5\lambda+2}. \tag{54}$$

By rewriting each variable to the original one, one obtains the kink solution of the headway:

$$\triangle x_n=h_c\pm\sqrt{-\frac{10(3\lambda+1)V'}{(5\lambda+2)V'''}\left|\frac{a_c}{a}-1\right|}$$
$$\times\tanh\left\{\sqrt{\frac{5\left|\frac{a_c}{a}-1\right|}{5\lambda+2}}\left[n+\left(1-\frac{5(3\lambda+1)}{3(5\lambda+2)}\left|\frac{a_c}{a}-1\right|\right)V't\right]\right\}. \tag{55}$$

When $\lambda=0$, $C=5$ is the result derived from the OVM [10, 11, 16].

3. Simulation

Since equations (19), (39) and (55) have predicted the triangular shock, soliton and kink–antikink waves in respective region, we hope we can realize them in numerical simulations with equation (2) and the optimal velocity function

$$V(\triangle x_n)=\frac{v_{\max}}{2}\{\tanh(\triangle x_n-h_c)+\tanh(h_c)\}, \tag{56}$$

where $v_{\max}$ is the free flow velocity and h_c is the safe distance [3, 15]. Applying the finite difference method to discretize equation (2), one obtains the following difference update rules:

$$v_n(t+\triangle t)=v_n(t)+\triangle t\{a[V(x_{n+1}(t)-x_n(t))-v_n(t)]+\lambda a[v_{n+1}(t)-v_n(t)]\}, \tag{57}$$

$$x_n(t+\triangle t)=x_n(t)+\triangle t\frac{v_n(t+\triangle t)+v_n(t)}{2}. \tag{58}$$

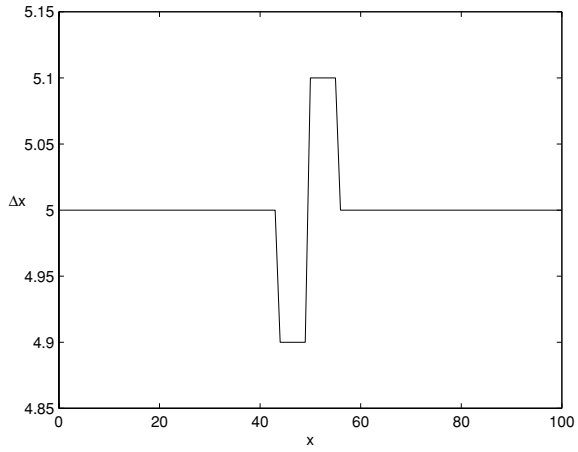

Figure 1. The initial perturbation I.

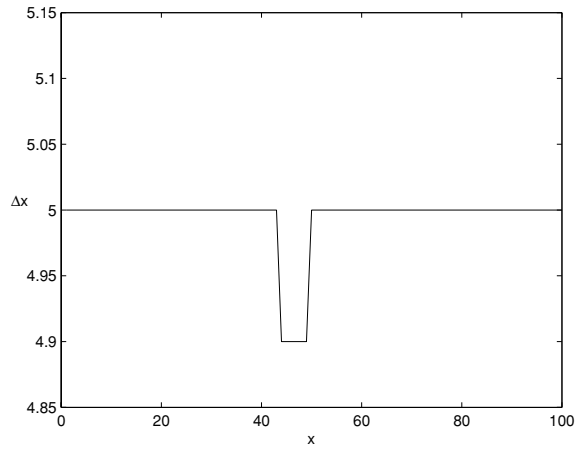

Figure 2. The initial perturbation II.

We adopt two initial perturbations I and II as follows (figures 1 and 2):

$$x_n(0) = \begin{cases} x_{n-1}(0) + h_c - \delta x & n_1 < n < n_2, \\ x_{n-1}(0) + h_c + \delta x & n_2 < n < n_2 + n_2 - n_1, \\ x_{n-1}(0) + h_c & \text{other} \quad n \in [0, N], \end{cases} \tag{59}$$

$$x_n(0) = \begin{cases} x_{n-1}(0) + h_c - \delta x & n_1 < n < n_2, \\ x_{n-1}(0) + h_c & \text{other} \quad n \in [0, N], \end{cases} \tag{60}$$

$$v_n(0) = V(\triangle x^{(0)}). \tag{61}$$

We take the number of the cars $N = 100$, $\triangle t = 0.1$ s, $n_1 = 45$, $n_2 = 50$, $v_{\max} = 2.0$ m s^{-1} and $\lambda = 0.5$.

When $a = 0.5$ s^{-1}, $h_c = 5.0$ m and $\triangle x^{(0)} = 5.0$ m, the stability criterion, equation (7), cannot be satisfied and the initial perturbation is unstable. Figure 3 shows that the initial perturbation I with $\delta x = 0.1$ in figure 1 can evolve to the kink waves after enough time, which confirms the existence of the kink solution, equation (55), in the unstable region within the

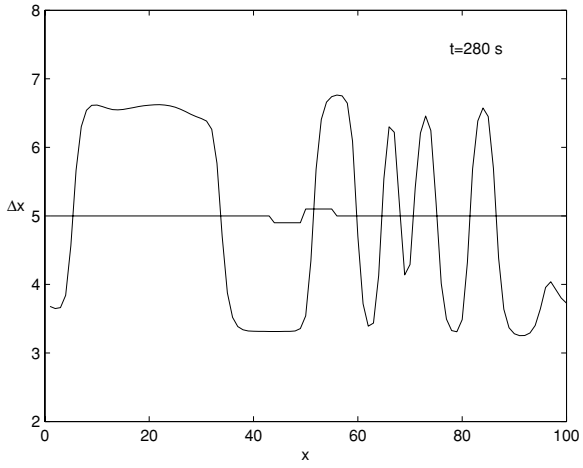

Figure 3. Kink wave.

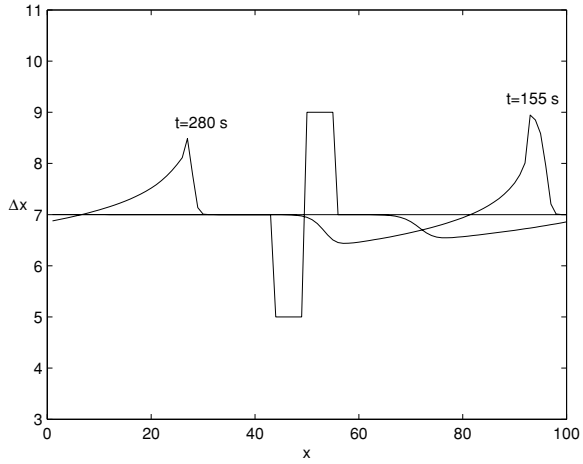

Figure 4. Triangular shock wave.

spinodal line. We can get the same numerical result as figure 3 with the initial perturbation II, which implies that the kink waveform in the unstable region may be independent of the initial perturbation configuration. This conclusion has also been obtained by the fluid dynamic model [21].

When $a = 0.5\ \mathrm{s}^{-1}$, $h_c = 5.0$ m and $\triangle x^{(0)} = 7.0$ m, the stability criterion, equation (7), can be satisfied and the initial perturbation is stable. Figure 4 shows that the initial perturbation I with $\delta x = 2.0$ in figure 1 can evolve to the triangular shock wave during the relaxation process of the nonuniform flow to the uniform steady flow, which confirms the existence of the triangular shock solution, equation (19), in the stable region out of the coexisting line. However, there is no triangular shock wave either in figure 5 beginning from the initial perturbation II with $\delta x = 2.0$ or in figure 6 beginning from the initial perturbation I with $\delta x = 0.5$, that is to say, the triangular shock wave appears only from the strong positive initial perturbation in the free flow, the physical significance of which is evident: when small or negative perturbation happens in the free flow, the car with the velocity less

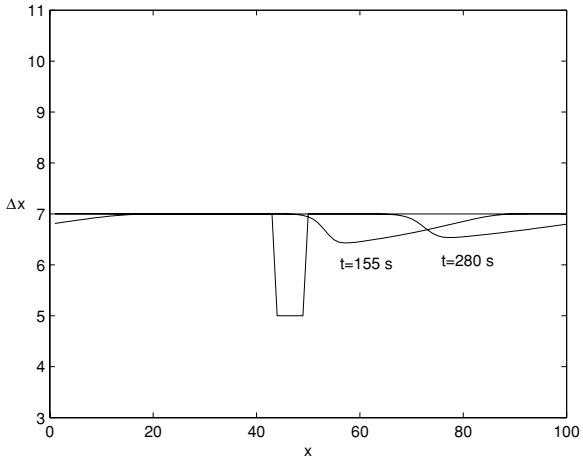

Figure 5. Perturbation propagation.

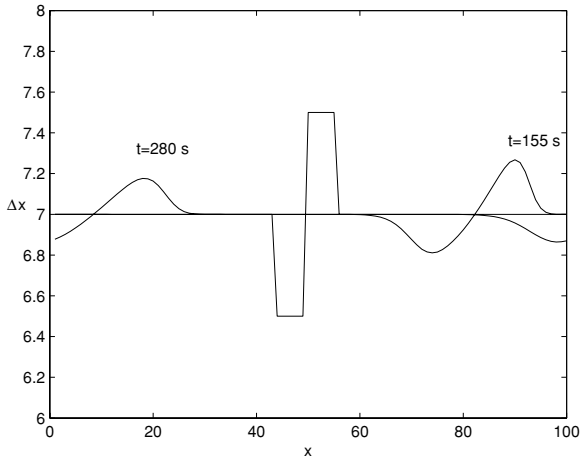

Figure 6. Perturbation propagation.

than the optimal velocity and the headway less than the average headway in the perturbation region will accelerate to the optimal velocity, and then the traffic flow becomes homogeneous and stable again. However, when a large positive perturbation happens, it is not necessary that the cars with the optimal velocity and the headway larger than average headway in the perturbation region decelerate to a velocity less than the optimal velocity or the cars outside the perturbation region accelerate to a velocity larger than the optimal velocity since all cars run with the optimal velocity, and therefore the strong headway interruption profile always exists during the relaxation process of the nonuniform flow to the uniform steady flow.

Substituting $h_c = 3.0$ m, $\triangle x^{(0)} = 4.0$ m, $v_{max} = 2.0$ m s^{-1} and $\lambda = 0.5$ into the spinodal line $a_s = \frac{2}{2\lambda+1}V'$, we get $a_s = 0.42$. Figure 7 shows that the initial perturbation II with $a = 0.45$ s^{-1} and $\delta x = 0.1$ in figure 2 can slowly dissipate to the static soliton wave, which confirms the existence of the soliton solution, equation (39), near the spinodal line. However, figure 8 shows that the initial perturbation I with $a = 0.45$ s^{-1} and $\delta x = 0.1$ in figure 1 produces a sine wave but not a soliton, that is to say, different initial conditions will

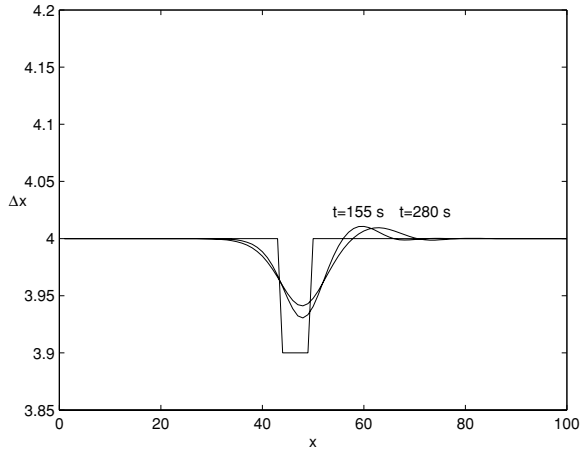

Figure 7. Soliton wave.

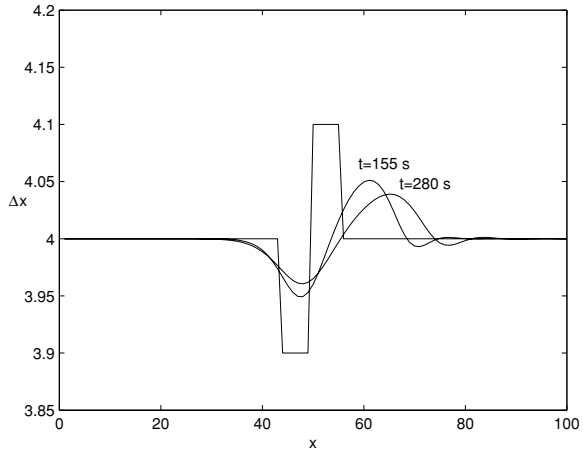

Figure 8. Sine wave.

produce different waveforms near the spinodal line. Both soliton and sine waves appearing near the spinodal line have small propagation velocity and stay statically in the initial location. This quality of soliton is similar to the synchronized flow: once the synchronized flow has occurred at an on-ramp, the downstream front of the synchronized flow is fixed at the on-ramp. Moreover, the kink wave also possesses some characteristics of wide moving jam [22], e.g., the propagation velocity and the flux on the outflow. It can be considered that nonlinear wave theory has inner relations with three-phase traffic flow theory, though the latter has much more complicated structure than the former.

4. Summary

We have analysed the FVDM and derived the Burgers, KdV and MKdV equations, respectively, in the stable region out of the coexisting curve, near the spinodal line and in the unstable region within the spinodal line. We have obtained the triangular shock, soliton and kink–antikink

solutions analytically. The triangular shock, soliton and kink–antikink density waves are described, respectively, by the Burgers, KdV and MKdV equations. The equations and solutions from the FVDM can be reduced to those from the OVM if not considering the effect of velocity difference. The numerical simulations confirm the existence of the triangular shock wave, the soliton wave and the kink–antikink wave in respective region. The triangular shock wave and the soliton wave can only be produced under certain initial condition. Only strong positive perturbation can yield the triangular shock wave in free flow and the strong headway interruption profile happens during the relaxation process of the nonuniform flow to the uniform steady flow. The soliton wave is fixed at the initial location, which is similar to the synchronized flow with respect to the spatial limit. We can further find more similarities between the nonlinear flow theory and three-phase traffic flow theory.

Acknowledgments

This work was financially supported by the Chinese National Science Foundation with grant no 10532060.

References

[1] Nagel K and Schreckenberg M 1992 *J. Phys.* I **2** 2221
[2] Bando M, Hasebe K, Nakayama A, Shibata A and Sugiyama Y 1994 *Japan. J. Ind. Appl. Math.* **11** 203
[3] Bando M, Hasebe K, Nakayama A, Shibata A and Sugiyama Y 1995 *Phys. Rev.* E **51** 1035
[4] Bando M, Hasebe K, Nakanishi K, Nakayama A, Shibata A and Sugiyama Y 1995 *J. Phys. I (France)* **5** 10389
[5] Kerner B S, Konhäuser P and Schilke M 1995 *Phys. Rev.* E **51** 6243
[6] Kerner B S and Rehborn H 1996 *Phys. Rev.* E **53** R1297
[7] Kerner B S and Konhäuser P 1993 *Phys. Rev.* E **48** 2335
[8] Kurtze D A and Hong D C 1995 *Phys. Rev.* E **52** 218
[9] Komatsu T and Sasa S 1995 *Phys. Rev.* E **52** 5574
[10] Muramatsu M and Nagatani T 1999 *Phys. Rev.* E **60** 180
[11] Nagatani T 2000 *Phys. Rev.* E **61** 3564
[12] Nagatani T, Nakanishi K and Emmerich H 1998 *J. Phys. A: Math. Gen.* **31** 5431
[13] Nagatani T 1998 *Physica* A **261** 599
[14] Nagatani T and Nakanishi K 1998 *Phys. Rev.* E **57** 6415
[15] Nagatani T 1998 *Phys. Rev.* E **58** 4271
[16] Nagatani T 2002 *Rep. Prog. Phys.* **65** 1331–86
[17] Helbing D and Tilch B 1998 *Phys. Rev.* E **58** 133
[18] Jiang R, Wu S W and Zhu Z J 2001 *Phys. Rev.* E **64** 017101
[19] Cross M C and Hohenberg P C 1993 *Rev. Mod. Phys.* **65** 851
[20] Tatsumi T and Kida S 1972 *J. Fluid Mech.* **55** 659
[21] Kerner B S and Konhäuser P 1994 *Phys. Rev.* E **50** 54
[22] Kerner B S 2002 *Math. Comput. Modelling* **35** 481–508